Photochemical Reaction Mechanisms of β,γ-Unsaturated Ketones. The 1,3-Acetyl Shift in Cyclopent-2-enyl Methyl Ketones

David E. Sadler, Joachim Wendler, Gottfried Olbrich, and Kurt Schaffner*

Contribution from the Max-Planck-Institut für Strahlenchemie, D-4330 Mülheim a. d. Ruhr, West Germany. *Received September 8, 1983*

Abstract: The topological course of the photochemical 1,3-acetyl shift in (*R*)-(+)-cyclopent-2-enyl methyl ketones and the kinetics of the processes deactivating the fluorescent $S_1(n,\pi^*)$ state have been studied. The reaction is shown to proceed in a predominantly suprafacial manner to form the rearranged (*S*)-(−)-isomer. Independent of the temperature in the range of −45 to +50 °C, an upper limit of only about 20% of the reaction occurs with racemization. These results, in conjunction with those of a previous CIDNP study, are explained by a mechanism in which the 1,3-acetyl shift proceeds at least in part via a radical pair by α-cleavage from the $S_1(n,\pi^*)$ and $T_2(n,\pi^*)$ excited states. The dominating reaction throughout the temperature range studied is, however, from S_1, either concerted or via the radical pair, even though the proportion of the T_2 radical cleavage increases with decreasing temperature. A combination of fluorescence lifetime and reaction quantum yield studies as a function of temperature and solvent polarity disclosed two thermal activation barriers deactivating $S_1(n,\pi^*)$, the larger one of which is shown to be associated with the 1,3 shift. The results of semiempirical calculations of the electronic structures of the excited states of 1,2-dimethylcyclopent-2-enyl methyl ketone at or very near to the equilibrium geometry were in full accord with the stereochemistry- and multiplicity-dependent mechanistic scheme.

The photochemistry of β,γ-unsaturated ketones (β,γ-UKs) has recently been extensively reviewed.[1] It is characterized by two predominant reactions: the oxadi-π-methane (ODPM) rearrangement and the allylic 1,3-acyl shift (1,3-AS). Cyclopent-2-enyl methyl ketones such as **1** (Scheme I) were among the first examples with which this typical behavior of β,γ-UKs was documented.[2] The 1,3-AS to **2** prevails on direct excitation and has been found to proceed from both the S_1 and $T_2(n,\pi^*)$ states,[2d-f,3] whereas the ODPM rearrangement to **3** predominates upon triplet sensitization of the cylopentenyl methyl ketones and has been shown to occur from the lowest-lying triplet state, $T_1(\pi,\pi^*)$.[2a-e]

Photo-CIDNP and radical trapping experiments[2f] have shown that the 1,3-AS of the cyclopentenyl methyl ketones must, at least in part, be a radical process, proceeding predominantly via a cage radical pair (RP) which also gives rise to disproportionation products such as acetaldehyde and diene. The inversion of the CIDNP polarizations which occurs on changing the temperature was explained, in terms of the radical pair mechanism for CIDNP,[4] by suggesting that the RP is predominantly formed from a singlet excited state, $S_1(n,\pi^*)$, in the high-temperature region (e.g., +50 °C for **1**) and from a triplet state, $T_2(n,\pi^*)$, in the low-temperature region (e.g., −50 °C for **1**).[2f,6] Temperature-activated α-cleavage from S_1 was postulated to explain this change in the multiplicity of the reactive excited state with temperature.[2f]

Scheme I. Predominant Reaction Pathways on Direct and Sensitized Irradiation of the β,γ-Unsaturated Ketones **1a-d**

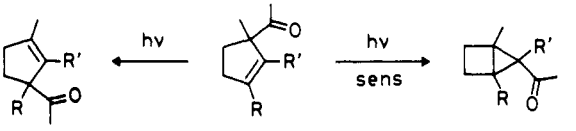

2 **1** **3**

a, R = R' = H; b, R = H, R' = CH_3; c, R = R' = CH_3; d, R = CD_3, R' = CH_3

We report now on further studies of the 1,3-AS in ketones of type **1** in a continuation of our systematic investigation of this particular β,γ-UK system.[7] It will be shown that the photo-CIDNP effects described previously[2f] reflect the mechanism operative in the overall reaction, although only a small proportion of the reaction results in polarized products. In addition to the importance of the RP pathway, the responses of the excited-state deactivation modes to changes in the environmental conditions will be discussed.

The Stereochemical Course of the 1,3-Acetyl Shift

The observation of CIDNP effects established qualitatively that radical pair recombination mechanisms contribute to the 1,3-AS in β,γ-UKs of type **1**. However, a quantitative assessment of the importance of the radical pathway relative to other possible routes leading to the same product is not readily obtained from CIDNP experiments.[8] Experiments with enantiomerically enriched **1d** and **2d** were designed in order to determine the stereochemical course of the 1,3-AS, and thus to provide quantitative information on the importance of the RP pathway.

In order to generate magnetic nuclear polarization in the cage products, the radical pair mechanism for CIDNP[4] requires that the components of the RP diffuse far enough apart to render the electron exchange energy small relative to the electron-nuclear hyperfine interactions (typically 6–10 Å, i.e., solvent separated[5b]) and then to undergo intersystem crossing (in competition with complete separation of the radical pair) before undergoing secondary geminate recombination.[9] For typical organic radicals

(1) (a) Schuster, D. I. In "Rearrangements in Ground and Excited States"; de Mayo, P., Ed.; Academic Press: New York, 1980; Vol. 3, p 167.

(2) (a) Baggiolini, E.; Schaffner, K.; Jeger, O. *Chem. Commun.* **1969**, 1103. (b) Tegmo-Larsson, I.-M.; Gonzenbach, H.-U.; Schaffner, K. *Helv. Chim. Acta* **1976**, *59*, 1376. (c) Gonzenbach, H.-U.; Tegmo-Larsson, I.-M.; Grosclaude, J.-P.; Schaffner, K. *Ibid.* **1977**, *60*, 1091. (d) Schaffner, K. *Tetrahedron* **1976**, *32*, 641. (e) Mirbach, M. J.; Henne, A.; Schaffner, K. *J. Am. Chem. Soc.* **1978**, *100*, 7127. (f) Henne, A.; Siew, N. P. Y.; Schaffner, K. *Ibid.* **1979**, *101*, 3671; *Helv. Chim. Acta* **1979**, *62*, 1952.

(3) Dalton, J. C.; Shen, M.; Snyder, J. J. *J. Am. Chem. Soc.* **1976**, *98*, 5023. Schuster, D. I.; Eriksen, J.; Engel, P. S.; Schexnayder, M. A. *Ibid.* **1976**, *98*, 5025.

(4) For an introduction to the radical pair mechanism see ref 5a–d.

(5) (a) Closs, G. L. *Pure Appl. Chem., Spec. Lect.* **1971**, *4*, 19. (b) Turro, N. J. "Modern Molecular Photochemistry"; Benjamin/Cummings: Menlo Park, 1978; p 273. (c) Lepley, A. R.; Closs, G. L., Ed. "Chemically Induced Magnetic Polarization"; Wiley: New York, 1973. (d) Kaptein, R. In "Advances in Free Radical Chemistry"; Williams, G. H., Ed.; Elek Science: London, 1975; Vol. V, p 321. (e) Buchachenko, A. L. *Russ. Chem. Rev.* **1976**, *45*, 761. (f) Turro, N. J.; Kraeutler, B. *Acc. Chem. Res.* **1980**, *13*, 369.

(6) See ref 2e for the configurational assignments of the T_1 and T_2 states which undergo the ODPM rearrangement and the 1,3-AS, respectively, in cyclopentyl methyl ketones.

(7) Part of this work has been published in preliminary form: Sadler, D. E.; Hildenbrand, K.; Schaffner, K. *Helv. Chim. Acta* **1982**, *65*, 2071.

(8) Lawler, R. G. In "Chemically Induced Magnetic Nuclear Polarization"; Muus, L. T., Atkins, P. W., McLauchlan, K. A., Pedersen, J. B., Eds.; Reidel: Dordrecht, Boston, 1977; p 275.

0002-7863/84/1506-2064$01.50/0

Scheme II. Mechanistic Routes for the Photochemical 1,3-Acetyl Shift Starting with Ketones (+)-1d and (−)-2d: The Concerted Enantiospecific Reaction and the Stepwise Pathway via α Cleavage to the Radical Pair (RP) (note that our experiments have been carried out with samples enriched with (+)-1d and (+)-2d)

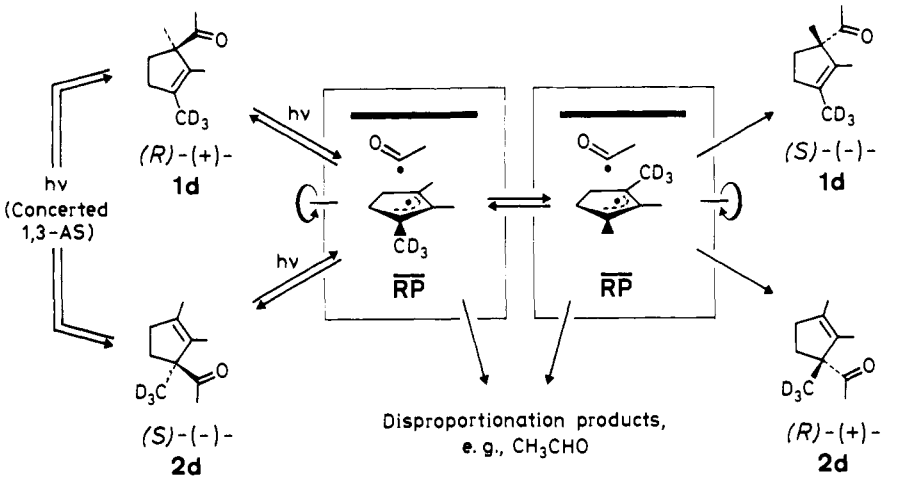

Scheme III. Synthesis of the Racemic Ketones 1d and 2d

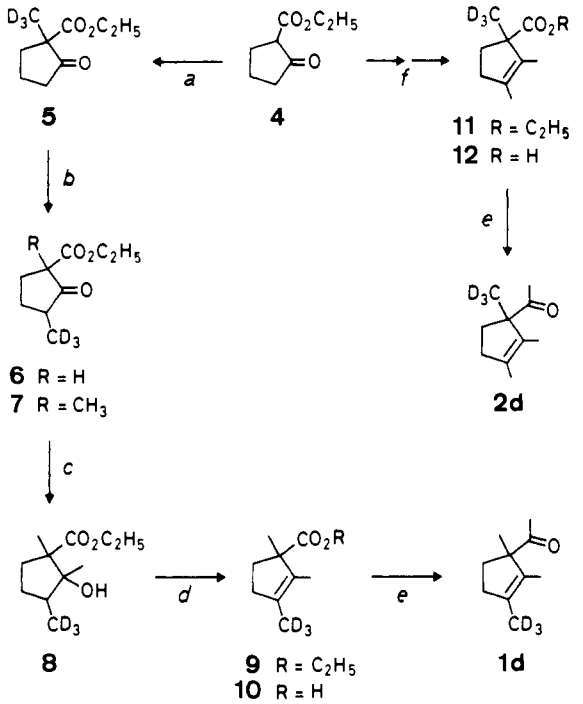

(a) CD_3I, *t*-BuOK, *t*-BuOH. (b) Na, C_2H_5OH, toluene (5→6); CH_3I, *t*-BuOK, *t*-BuOH (6→7). (c) CH_3MgI, ether. (d) *p*-Toluenesulfonic acid, benzene (8→9); KOH, aqueous CH_3OH (9→10). (e) CH_3Li, ether. (f) Reference 14 (4→11); see the experimental part for an improved and shorter procedure; KOH, aqueous CH_3OH (11→12).

Scheme IV. Resolution of Ketones (±)-1d and (±)-2d into Their Enantiomers

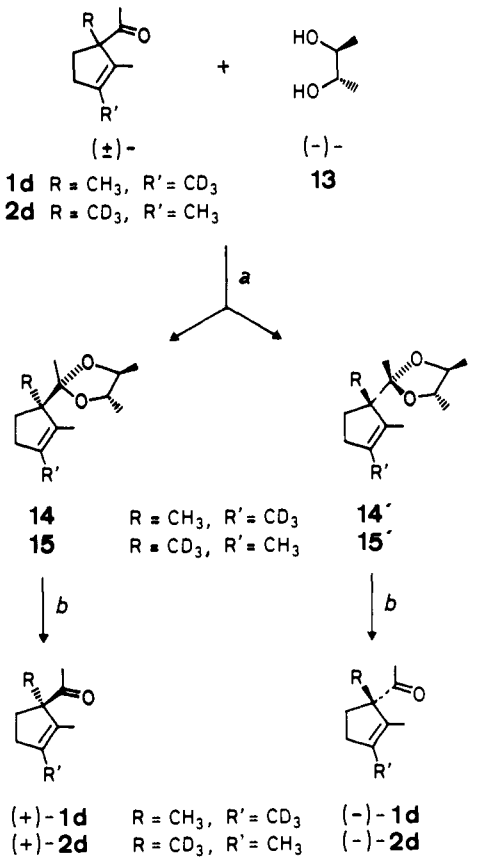

(a) *p*-Toluenesulfonic acid, benzene. (b) Aqueous HCl, EtOH.

intersystem crossing can take place on a time scale as short as ca. 10^{-9} s.[5,10] However, rotation of the cyclopentenyl component by 180° about the axis indicated in Scheme II is expected to occur faster, i.e., on a time scale of ca. 10^{-12} to 10^{-11} s.[11]

Starting with any one enantiomer, formation of both (+)- and (−)-**1d** and (+)- and (−)-**2d** has thus to be expected for a reaction

(9) Noyes, R. M. *J. Am. Chem. Soc.* **1955**, *77*, 2042.

(10) In the CIDNP experiments, which were conducted in a high field (H = 21 140 G), intersystem crossing ($S \leftrightarrow T_0$) in the RP due to Δg (≈ 0.0021[2f]) occurs on a time scale of the order of 8×10^{-9} s (see ref 5b, p 371). This figure will be modulated by the different electron–nuclear hyperfine interactions in each RP. In the low-field extreme (e.g., earth's magnetic field), intersystem crossing ($S \leftrightarrow T_-, T_0, T_+$) will be occasioned solely by the hyperfine interactions. Estimates of the magnitude of these interactions (Bennet, A. In "Landolt-Bornstein. Magnetic Properties of Free Radicals"; Fischer, H., Hellwege, K.-H., Eds.; Springer: Berlin, 1977; New Series, Vol. 9b, p 342) allow an upper limit of ca. 2×10^{-9} s for the time scale of this process. Under the irradiation conditions for **1d** and **2d**, i.e., a weak magnetic field due to the stirrer, the rate of intersystem crossing should be less than in either of the two extreme cases (see ref 5e,f for an explanation and some of the possible applications of this effect).

(11) Measurements of the rates of rotational diffusion of cyclohexane, cyclohexene, and benzene in solution show that these molecules undergo a 180° tumbling motion about a C_2 axis on a time scale of the order of 10^{-12} to 10^{-11} s at viscosities corresponding to those in methanol between +50° (0.4 cP) and −50° (2.2 cP): Tanabe, K. *J. Phys. Chem.* **1982**, *86*, 319; *Chem. Phys. Lett.* **1981**, *83*, 397. Pajak, Z.; Latanowicz, L.; Jurga, K. *Ber. Bunsenges. Phys. Chem.* **1980**, *84*, 769. Tanabe, K.; Hiraishi, J. *Mol. Phys.* **1980**, *39*, 493.

Table I. Enantiomeric Composition of Ketone **1d** Resulting from the Irradiation in Methanol of Mixtures of **1d** and **2d** Enriched in the (*R*)-(+) Enantiomer

	irradiation of 84.3% (*R*)-(+)-**1d**, 15.7% (*S*)-(−)-**1d**[a]		irradiation of 86.0% (*R*)-(+)-**2d**, 14.0% (*S*)-(−)-**2d**[a]	
temp of irrad soln, °C	% conversion **1d** → **2d**	% (*S*)-(−)-**1d** after irrad	% conversion **2d** → **1d**	% (*R*)-(+)-**1d** formed by irrad
		[15.7 ± 2.0[b]]		[14.0 ± 2.0[c]]
+50	18.7	17.7	11.6	18.9
+50	22.7	15.0		
+20	13.1	18.9	11.9	16.5
+20	22.6	19.1	23.2	18.5
−10	10.0	17.1	10.3	18.6
−10	25.2	15.6	22.0	20.8
−45	11.4	16.4	11.0	16.6
−45	26.8	16.1	14.6	17.1

[a] Determined for **1d** by ^{1}H NMR with Pr(hfc)$_3$ and for **2d** by GC (70-m PPG glass capillary column) of the mixture of diastereoisomeric acetals before hydrolysis to the ketone. Using **1d**, the two methods gave the same result within ±2%; see Experimental Section. [b] Before irradiation: value given for comparison with the values after irradiation. [c] Percentage of (*S*)-(−)-**2d** before irradiation, given for comparison with the percentage values of (*R*)-(+)-**1d**. Note that the percentage of (+) component exceeding that originating from (*S*)-(−)-**2d** corresponds to racemization through a radical pair.

via the RP which leads to polarized products. In contrast, a mechanism in which the acetyl group remains on the same face of the cyclopentenyl group would be enantiospecific, leading to interconversion of either (+)-**1d** and (−)-**2d** or (−)-**1d** and (+)-**2d**. An orbital symmetry-allowed concerted 1,3-AS or a reaction in which recombination of the RP is faster than rotation of the cyclopentenyl radical would be examples of such a mechanism.

Preparation, Enantiomeric Resolution, and Analysis of Ketones 1 and 2. The deuterium-labeled ketones **1d** and **2d** were synthesized from **4** and **11**, respectively, as outlined in Scheme III. Similar synthetic sequences have already been used previously in the preparation of the nondeuterated ketone **1c**.[2c,12,13] The resolution of the racemic products **1d** and **2d** was accomplished by column chromatographic separation of the diastereoisomeric mixtures of acetals, **14**/**14′** and **15**/**15′**, formed with (−)-butane-2,3-diol (**13**) (Scheme IV). The absolute configurations of the optically active ketones **1d** and **2d** (enantiomeric composition ca. 70% + 30%) as displayed in the scheme were deduced from the signs of their optical rotations.[2a,15] With the aid of an optishift reagent, the ^{1}H NMR signals of the quaternary methyl groups of (+)-**1d** and (−)-**1d** could be separated and integrated. Thus, three analytical figures were available: ^{1}H NMR giving the ratio **2d**/**1d**, ^{1}H NMR optishift giving the ratio (+)-**1d**/(−)-**1d**, and optical rotation giving the ratio (+)-(**1d** + **2d**)/(−)-(**1d** + **2d**). The last figure could alternatively be determined by GC analysis of the ratio of the diastereoisomeric acetals (**14** + **15**)/(**14′** + **15′**). This allowed a complete analysis of the four-component mixture (+)-**1d**, (−)-**1d**, (+)-**2d**, and (−)-**2d**, resulting from photolytic α cleavage and back reaction (**1** ⇌ RP) and the 1,3-AS (**2** → **1**).

Irradiation Experiments with the Enantiomerically Enriched Ketones 1d and 2d. The experiments with (+)-enriched **1d** (Table I) in CH_3OH show that the starting material does not noticeably racemize upon irradiation in the temperature range −45 to +50 °C. Since **1d** is the starting material, however, even a fairly sizable loss of optical purity in the **1d** regenerated from the RP would not cause a detectable change in the overall enantiomeric ratio.[16] This limitation does not apply to the formation of **1d** on irradiation of **2d**. The results obtained with (+)-enriched **2d** do indeed show a small change in the enantiomeric composition of the 1,3-AS product (**1d**) as compared with the starting material, independent of the temperature in the range studied, although this change is on the border of our experimental accuracy. Only an upper limit of approximately 20% reaction with racemization, i.e., a maximum of about 20% reaction through an RP which yields polarized products, can be calculated from the results in Table I.

These results, in conjunction with those of the CIDNP experiments,[2f] may be explained by a mechanism in which (i) the 1,3-AS proceeds at least in part via RP, (ii) α cleavage does occur from both the $S_1(n,\pi^*)$ and $T_2(n,\pi^*)$ excited states, and (iii) the proportion of the T_2 reaction indeed increases with decreasing temperature. It requires, however, that reaction from S_1, either concerted or via RP, dominate throughout the temperature range studied and that, if the dominating S_1 pathway is via RP rather than concerted, rotation of the cyclopentenyl radical in the RP as shown in Scheme *II is slow compared to product formation.*

Thus, at +50 °C the effect of the T_2 reaction is assumed to be negligible. The singlet radical pair, ^{1}RP, formed from S_1, will predominantly undergo rapid primary geminate recombination (10^{-13}–10^{-11} s)[9] to yield unpolarized (no CIDNP) disproportionation and recombination products,[5] in competition with separation of the radicals by diffusion. Primary geminate recombination could even be faster than rotation of the cyclopentenyl radical about its in-plane axis (see Scheme II; molecular tumbling is estimated to proceed at 10^{-12}–10^{-11} s),[11] allowing for highly enantioselective interconversions, (+)-**1d** ⇌ (−)-**2d** and (−)-**1d** ⇌ (+)-**2d**. A concerted contribution, which would be required to proceed in the suprafacial manner, would also be enantiospecific and give rise to no CIDNP effect. Radicals which have diffused apart can still react with each other (secondary geminate recombination).[9] The observed singlet CIDNP must then be due to the small proportion of radicals reacting by this mechanism on a time scale of ca. 10^{-9}–10^{-7} s. The racemization (for **2** ⇌ **1**) at +50 °C is the result of both secondary geminate recombinations and random reaction of free radicals (i.e., uncorrelated pairs).[17]

Since the ^{3}RP has to undergo intersystem crossing prior to reaction, most of the ^{3}RP will live long enough to be able to contribute to CIDNP. *A small proportion of the T_2 reaction will therefore suffice to cause a polarization intensity equal to or greater than that of the singlet CIDNP.*[18]

As the temperature is lowered from +50 °C (where the effect of the T_2 reaction is postulated to be negligible), the proportion of the T_2 reaction increases: at ca. −5 °C, it produces a triplet polarization of sufficient intensity to cancel out the singlet contribution, and at −45 °C it leads to a pronounced triplet CIDNP spectrum although the proportion of the T_2 reaction is still small,[19] reaction from S_1 dominating.

(12) Meyer, W. L.; Lobo, A. P.; Marquis, E. T. *J. Org. Chem.* **1965**, *30*, 181.

(13) For an alternative preparation of **2d** via the aldehydic precursor see ref 2a and 14.

(14) Baggiolini, E.; Hamlow, H. P.; Schaffner, K. *J. Am. Chem. Soc.* **1970**, *92*, 4906.

(15) Snatzke, G.; Schaffner, K. *Helv. Chim. Acta* **1968**, *51*, 986.

(16) For the purposes of comparison it can be calculated that, for a reaction solely via a long-lived RP, an enantiomeric composition of 24.3% (−)-**1d** and 75.7% (+)-**1d** would result on 20% conversion to the 1,3-AS product.

(17) The products resulting from reaction of uncorrelated pairs will be polarized (F pair polarization) in the opposite sense to those formed by secondary geminate recombination of the ^{1}RP. Since the specific polarization arising from the former is expected to be weaker than that due to the latter, no quantitative conclusions can be drawn about the relative importance of the two pathways.

(18) The specific polarization generated by triplet radical pairs is higher than that generated by singlet radical pairs (see ref 5c, p 101). This effect will have to be borne in mind in studies where photo-CIDNP is used to decide whether a singlet or a triplet excited state is reactive. A realistic picture of the radical pair processes, which can be observed by CIDNP, is given in Figure 4.

(19) Preliminary results of CIDNP experiments show that the proportion of T_2 reaction continues to increase as the temperature is lowered still further. The observed triplet polarizations [i.e., $(I_p/I_0)(t/T_1)$] for acetaldehyde and **1** (formed on irradiation of **2**) increase markedly on going from −40 to −80 °C.

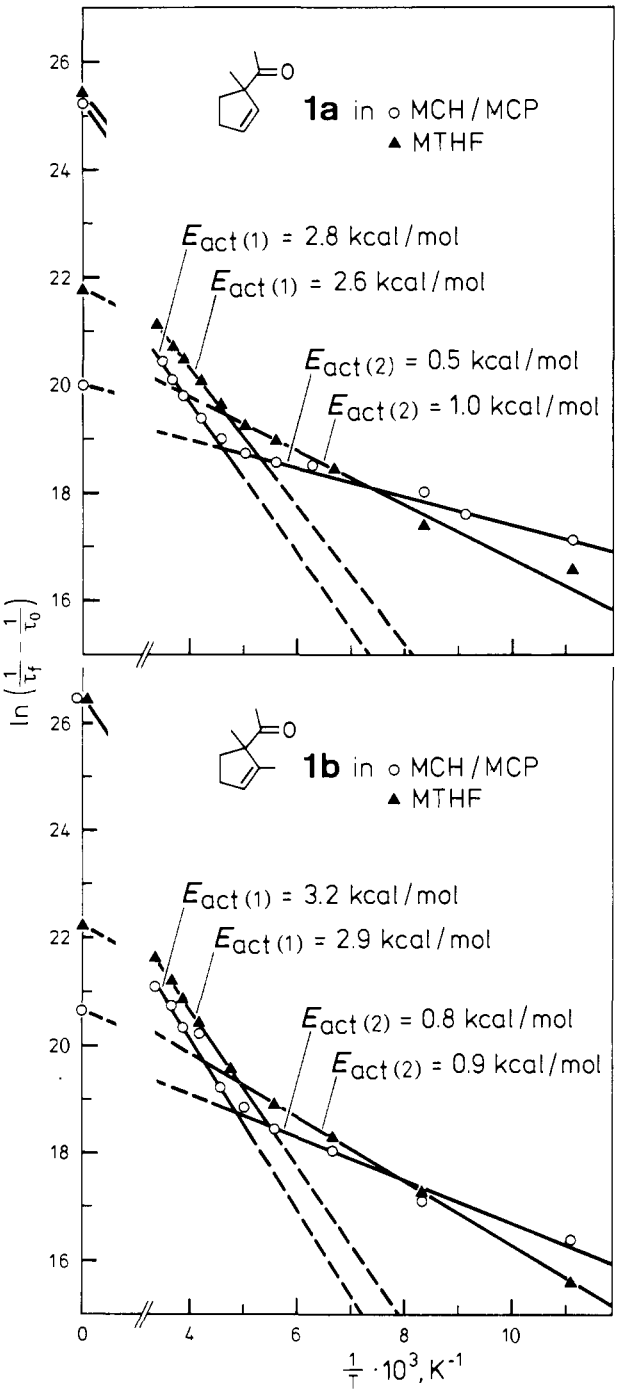

Figure 1. Arrhenius plots for the fluorescence lifetimes of ketones **1a** and **1b** in a 1:1 mixture of methylcyclohexane (MCH) and methylcyclopentane (MCP) and in 2-methyltetrahydrofuran (MTHF) (cf. Table II). The intercept values at $1/T = 0$ are extrapolations. For the τ_0 values see the Experimental Section.

Fluorescence Lifetime and Quantum-Yield Studies

The mechanism proposed above could be corroborated and the importance of the various pathways could be determined quantitatively if the rates of all the competing processes could be measured. Such kinetic data can be obtained for a photochemical reaction from excited-state lifetime and quantum-yield determinations.

A combination of fluorescence lifetime and reaction quantum-yield studies allowed the direct determination of the kinetics of the processes deactivating the fluorescent $S_1(n,\pi^*)$ excited state. However, it was not possible to determine the lifetimes of either of the reactive triplet states since neither phosphorescence nor triplet absorption could be detected. For the ODPM rearrangement from T_1, the data are thus restricted to quantum yields,

Table II. Activation Parameters for the Fluorescence Lifetimes of the Ketones **1a**, **1b**, and **1c**[a]

		large activation barrier		small activation barrier	
ketone	solvent[b]	$E_{act(1)}$, kcal/mol	A_1, s^{-1}	$E_{act(2)}$, kcal/mol	A_2, s^{-1}
1a	MCH/MCP	2.8	9×10^{10}	0.5	5×10^{8}
	MTHF	2.6	1×10^{11}	1.0	3×10^{9}
1b	MCH/MCP	3.2	3×10^{11}	0.8	9×10^{8}
	MTHF	2.9	3×10^{11}	0.9	5×10^{9}
1c	MCH/MCP	2.9	6×10^{11}	0.7	2×10^{9}
	MTHF	2.8	7×10^{11}	1.2	9×10^{9}

[a] Determined for the temperature range 60-300 K; cf. Figure 1. [b] Abbreviations: MCH, methylcyclohexane; MCP, methylcyclopentane; MTHF, 2-methyltetrahydrofuran.

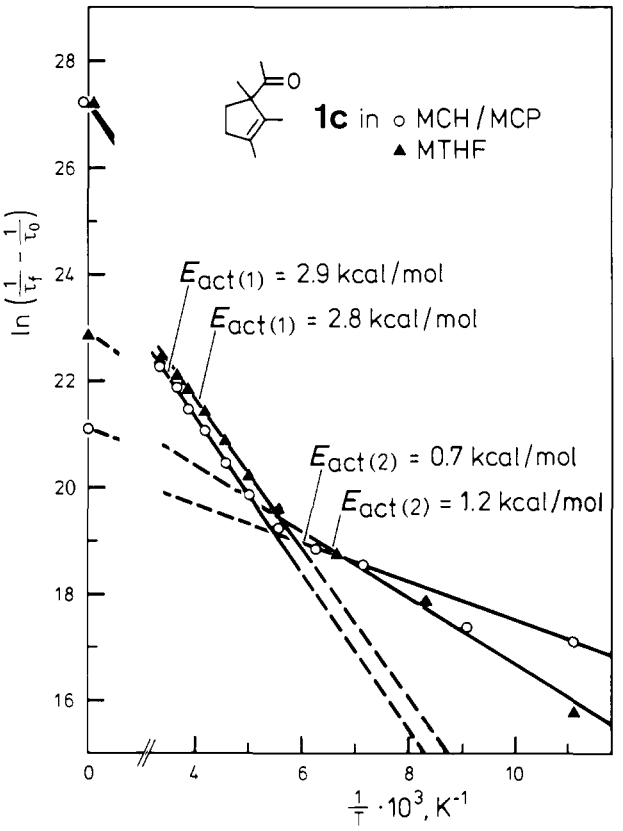

Figure 2. Arrhenius plot for the fluorescence lifetime of ketone **1c** in a 1:1 mixture of methylcyclohexane (MCH) and methylcyclopentane (MCP) and in 2-methyltetrahydrofuran (MTHF) (cf. Table II). The intercept values at $1/T = 0$ are extrapolations. For the τ_0 values see the Experimental Section.

and for the 1,3-AS from T_2, they are restricted to its contribution to the composite rate constant for the S_1 and T_2 reactions. Despite these limitations, a substantial body of mechanistic information has been derived for both the singlet and triplet processes.

The fluorescence lifetimes of **1a–c** were found to depend both on temperature and solvent polarity. Arrhenius plots indicate that in each case two processes with thermal activation barriers are deactivating $S_1(n,\pi^*)$ (Figures 1 and 2, and Table II). This result corroborates our proposal that such processes must exist in order to explain the increase in the T_2 reaction on lowering the temperature.[2f]

Comparison of the rates calculated from the E_{act} and A values (Table II) with the fluorescence lifetimes (Table III) shows that at and around room temperature the $S_1(n,\pi^*)$ photochemistry is dominated by the process with the large activation barrier ($E_{act(1)}$).[20] This is clearly illustrated also by Figures 1 and 2. The

Table III. Fluorescence Lifetimes of Ketones **1a**, **1b**, and **1c**; Dependence on Temperature and Solvent Polarity

ketone	solvent[a]	fluorescence lifetime (τ_f), ns, at +80 °C[b]	+50 °C[b]	+20 °C	−10 °C	−45 °C
1a	MCH/MCP	0.67	0.83	1.08	1.50	2.47
	MTHF	0.34	0.45	0.62	0.94	1.74
1b	MCH/MCP	0.36	0.47	0.64	0.96	1.77
	MTHF	0.20	0.28	0.41	0.66	1.34
1c	MCH/MCP	0.11	0.15	0.23	0.40	0.82
	MTHF	0.09	0.12	0.18	0.29	0.60

[a] Abbreviations: MCH, methylcyclohexane; MCP, methylcyclopentane; MTHF, 2-methyltetrahydrofuran. [b] The τ_f values at +50 and +80 °C were obtained from extrapolation of a plot of ln τ_f^{-1} vs. T^{-1}.

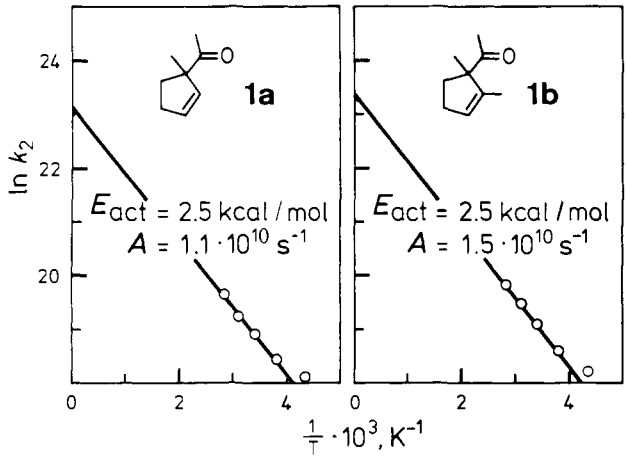

Figure 3. Arrhenius plots for the 1,3-AS of ketones **1a** and **1b** at 313 nm in isooctane. Note that the k_2s at 20 °C from these plots are practically identical with those obtained from Φ_2 and τ_f (Table IV), i.e., k_2 = 1.5 × 10^{-8} vs. 1.6 × 10^{-8} (for **1a**) and 2.1 × 10^{-8} vs. 2.0 × 10^{-8} s^{-1} (for **1b**).

decrease in fluorescence lifetimes seen on going from a hydrocarbon solvent to 2-methyltetrahydrofuran (Table III) shows, furthermore, that this process is dependent on the solvent polarity. The Arrhenius parameters (Table II) indicate that the increase in fluorescence decay rate with increasing solvent polarity is due to a decrease in the activation energy barrier, although the differences are too small to be measured accurately.

An examination of the temperature dependence of the quantum yields for reaction sheds light on the nature of this process. From the fluorescence lifetimes (Table III) and the quantum yields for the 1,3-AS reaction, Φ_2, (Table IV) the pseudo-first-order rate constant for the 1,3-AS reaction, k_2, can be calculated as a function of temperature for **1a** and **1b** in a hydrocarbon solvent (Table IV). Both sets of data fit simple Arrhenius plots (Figure 3), giving thermal activation barriers of E_{act} = 2.5 kcal/mol for the 1,3-AS of both **1a** and **1b** (with A = 1.1 × 10^{10} s^{-1} for **1a** and A = 1.5 × 10^{10} s^{-1} for **1b**). These values are comparable with those obtained for the process with the large activation barriers deactivating $S_1(n,\pi^*)$ (Table II), although both the E_{act} and A values obtained from k_2 are lower than those obtained from the fluorescence lifetime data. The differences may not lie outside the experimental error, but both the lower E_{act} and A values could, in fact, be meaningful. The Arrhenius parameters obtained from the fluorescence lifetime data (Figures 1 and 2) are, of course, the values for reaction from S_1 alone. However, according to our mechanism the k_2 values result from a composite of S_1 and T_2 reactions. The contribution from T_2 is proposed to increase with decreasing temperature. As the temperature is lowered the composite rate constant k_2 will be increasingly greater than the rate constant for the S_1 contribution alone. The E_{act} values obtained from the Arrhenius plots for k_2 (Figure 3) will thus be lower than those for the 1,3-AS from S_1 (Figure 1), as is found. The process with the large activation barrier deactivating S_1 can thus be equated with the pathway leading to the 1,3-AS product.

The lower A values are readily rationalized by postulating that the process deactivating S_1 with an activation barrier of $E_{act(1)}$ leads only in part to the 1,3-AS product. Thus, the rate constants (and the quantum yields, Table IV) for the 1,3-AS are only a fraction of the rate constants (and the quantum yields[20]) for the major process deactivating S_1 (Table V).

The picture of increasing triplet reactivity with decreasing temperature is supported by the increase in the quantum yields for the ODPM rearrangement (Table IV) as the temperature is lowered.

The effect of solvent polarity on the process leading to the 1,3-AS product is also reflected in the quantum yields for the ODPM rearrangement. Increasing the solvent polarity by going from a hydrocarbon solvent to 2-methyltetrahydrofuran (or methanol) increases the rate of the process with the large activation barrier (Table V) and leads to a decrease in the quantum yield

Table IV. Quantum Yields for Reaction of the Ketones **1a-c** and Pseudo-First-Order Rate Constants Obtained from Their Fluorescence Lifetimes and the Quantum Yields for the 1,3-AS to 2a-c

solvent[a]	temp, °C	quantum yields[b] Φ_{-1}	Φ_2	Φ_3	Φ_2/Φ_3	$k_2 \times 10^{-8}$,[c] s^{-1}
		Ketone **1a**				
C_8H_{18}	+80	0.70	0.226	0.036	6.3	3.4
C_8H_{18}	+50	0.73	0.187	0.047	4.0	2.25
C_8H_{18}	+20	0.74	0.177	0.067	2.6	1.6
C_8H_{18}	−10	0.67	0.152	0.087	1.7	1.0
C_8H_{18}	−45	0.86	0.186	0.120	1.6	0.75
MTHF	+20	0.64	0.230	0.033	7.0	3.7
		Ketone **1b**				
C_8H_{18}	+80	0.56	0.147	0.016	9.2	4.1
C_8H_{18}	+50	0.62	0.135	0.023	5.9	2.9
C_8H_{18}	+20	0.50	0.125	0.035	3.6	2.0
C_8H_{18}	−10	0.55	0.115	0.060	1.9	1.2
C_8H_{18}	−45	0.63	0.148	0.098	1.5	0.8
MTHF	+20	0.48	0.130	0.016	8.1	3.2
		Ketone **1c**				
CH_3OH	+50	0.30	0.091	0.0017	53.5	
CH_3OH	+20	0.22	0.096	0.0025	38.4	
CH_3OH	−10	0.24	0.084	0.0036	23.3	
CH_3OH	−45	0.30	0.093	0.0067	13.9	
C_8H_{18}	+20	0.12	0.088	0.0084	10.5	3.8

[a] Abbreviations: C_8H_{18}, isooctane; MTHF, 2-methyltetrahydrofuran. [b] Quantum yields for consumption of starting material (Φ_{-1}), 1,3-AS to 2a-c (Φ_2), and ODPM rearrangement to 3 (Φ_3). [c] Pseudo-first-order rate constant for the 1,3-AS to 2, calculated from Φ_2 and τ_f (Table III); $k_2 = \Phi_2/\tau_f$.

Table V. Pseudo-First-Order Rate Constants (k_{Arrh}) for the S_1 Deactivation of Ketones **1a-c** at 20 °C Obtained from the Arrhenius Activation Parameters (Figures 1 and 2). Comparison with the Rate Constants (k_2) Obtained from the Fluorescence Lifetimes of **1a-c** and the Quantum Yields for the 1,3-AS

ketone	solvent[a]	$k_{Arrh} \times 10^{-8}$,[b] s^{-1}	$k_2 \times 10^{-8}$,[c] s^{-1}	k_2/k_{Arrh}
1a	C_8H_{18}	7.6	1.6	0.21
1b	C_8H_{18}	12.8	2.0	0.16
1c	C_8H_{18}	2.6	3.8	0.09
1a	MTHF	11.8	3.7	0.31
1b	MTHF	21.3	3.2	0.15
1c	MTHF	58.9		

[a] C_8H_{18}, isooctane; MTHF, 2-methyltetrahydrofuran. [b] Calculated from $E_{act(1)}$ and A_1 (Table II); $k_{Arrh} = A_1 \times e^{-E_{act}/RT}$. [c] Values taken from Table IV.

(20) From $k_1 = A_1 e^{-E_{act(1)}/RT}$ (Table II) and τ_f (Table III) the quantum yield at 20 °C, $\Phi = k_1\tau_f$, for the process with the large activation barrier ($E_{act(1)}$) is in hydrocarbon solvents 0.82 (**1a**), 0.82 (**1b**), and 0.98 (**1c**), and in 2-methyltetrahydrofuran 0.73 (**1a**), 0.87 (**1b**), and 1.06 (**1c**).

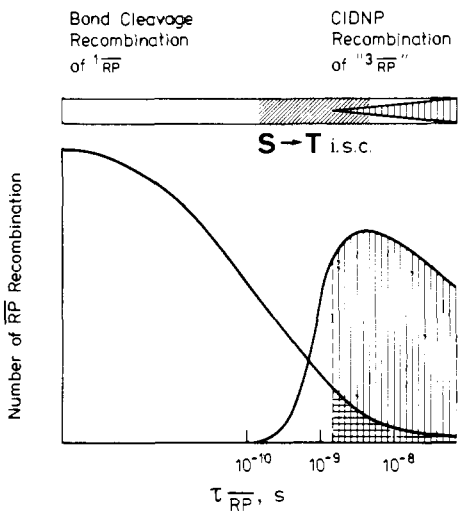

Figure 4. Top: Chronology of α cleavage and recombination of ^{1}RP radicals (blank area), S → T intersystem crossing (diagonal grid), and recombinations of the ^{3}RP and the F pair radicals (vertical grid). Bottom: Estimated proportions of non-CIDNP-polarized radical products (blank areas) and of those exhibiting singlet (horizontal grid) and triplet and F polarization (vertical grid).

for the ODPM rearrangement (Φ_3, Table IV). Comparison of the relative quantum yields for fluorescence in isooctane and 2-methyltetrahydrofuran (Table VI) shows that k_f ($=1/\tau_f + 1/\tau_0$) is unaffected by changes in solvent polarity, within experimental error.[21a]

We may finally note that the process with the small energy of activation deactivating S_1 ($E_{act(2)}$, Table II) shows an apparent increase in E_{act} on increasing the solvent polarity although the differences may lie within the experimental error. There is as yet no experimental evidence as to the nature of this process. One possibility is, inter alia, that it is associated with an orbital symmetry-allowed concerted 1,3-AS which competes, as a minor pathway to product, with the radical alternative.[21b]

Conclusion

The kinetic investigations described above lead to a picture of the mechanism for the photochemistry of the β,γ-UKs **1a–d** in which one temperature-activated process dominates the S_1 photochemistry at and around room temperature leading, in part, to the 1,3-AS and competing with fluorescence and intersystem crossing. Intersystem crossing populates both T_2, which undergoes the 1,3-AS, and T_1, which undergoes the ODPM rearrangement. The increase in the intersystem crossing yield on lowering the temperature is reflected both in increased quantum yields for the ODPM reaction and in the effect of the increasing contribution of the 1,3-AS from T_2 on the apparent energy of activation for the 1,3-AS reaction as a whole.

The predominance of singlet photochemistry is in accordance with the mechanism proposed to explain the results of the CIDNP and stereochemical studies described in this work, namely, that the triplet contribution to the 1,3-AS remains small throughout the temperature range studied.

The simplest description of the major process deactivating S_1 is a stretching of the allylic C(1)–CO bond leading to the 1,3-AS product either by a mechanism in which the C(3)–CO bond forms as the C(1)–CO bond breaks (a concerted process) or via α cleavage to the RP. Energy wastage could result from back reaction of the RP or via a deactivation channel associated with stretching of the C(1)–CO bond. The latter could simply be equated with a conventional vibronically coupled internal conversion mechanism. CNDO calculations suggest that just such a stretching motion is indeed a pathway deactivating S_1.

The 1,3-AS and ODPM Pathways. CNDO Calculations of the Excited States of Ketone 1b

Previous theoretical explorations into the possible reaction pathways of β,γ-UKs have been described by Schuster, Underwood, et al.,[22] who assumed different electron polarizations in the singlet and triplet excited states of the β,γ-UKs, and by Houk,[23] who carried out CNDO/S calculations. Some more extended calculations on the excited states of ketone **1b** have now been performed with the CNDO/S method of Del Bene and Jaffé[24] modified by the INDO integral approximation. This modification ensures proper splitting of $^1(n,\pi^*)$ and $^3(n,\pi^*)$ states. The geometry of the molecule was optimized with the CNDO/2 method, especially the geometry at C-1 and C-2 (cf. Scheme V).

Scheme V. Steric Views of Ketone **1b** Taken from Dreiding Models: **16A**, with the Planar Double Bond; **16B**, with the Double Bond Twisted around the C-2/C-3 Axis (out-of-plane twist ca. 15°)

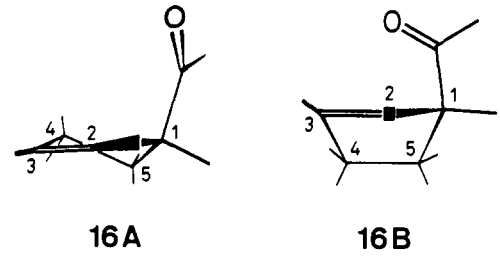

16A **16B**

The order of the lowest excited states calculated was $^3(\pi,\pi^*) < {}^3(n,\pi^*) < {}^1(n,\pi^*) < {}^1(\pi,\pi^*)$ with the very small interval of about 400 cm^{-1} between the two triplet states. Since the CNDO/S method is known to give too low energies for n,π^* states, one may assume a separation of the two states by an amount of several tenths of an electron volt. The classification of the states as n,π^* or π,π^* should not be taken literally, since appreciable charge-transfer character is always found.[23,25,26]

In order to elaborate further on the photochemical properties of the two lowest triplet states, an index was calculated characteristic for a given bond. This index was

$$\eta_{AB} = \sum_{r\in A}\sum_{s\in B} P_{rs}S_{rs}$$

which is proportional to the diatomic resonance energy contribution in the partitioning of the total energy.[27] The η_{AB} values should therefore be a qualitative measure for the bonding energy between atoms A and B. While the η_{CC} values for the C–C single bonds were calculated to lie in the range of 0.70–0.75 au, the value dropped to 0.67 au for the C(1)–CO bond in the n,π^* states. This is a significant change, the decrease amounting to ca. 30 au/mol. No such drastic change was found for any other C–C single bond. In the $^3(\pi,\pi)^*$ state there was a decrease in the η value of the C=C double bond from 1.06 to 0.83 au as one would expect. The change was accompanied by a very slight increase in the values of the C–C single bonds adjacent to the double bond. A concomitant increase of about 20% was also found for the value of $\eta_{C(2)-CO}$ which pertains to a formally nonbonded interaction, whereas for the ground state a very small bonding value of only 0.0087 au was calculated.

In a further set of calculations the C=C double bond of **16A** was twisted around an axis through C(5) and the midpoint of the double bond resulting in **16B**. The twisting was carried out in such a way as to shorten the distance C(2)–CO, and twist angles

(21) (a) An absolute quantum yield of Φ_f = ca. 9×10^{-4} has been reported for the fluorescence of ketone **1a** in CH_3CN.[2e] (b) **Note Added in Proof**: Irradiation experiments with **1b** in the gas phase (at, e.g., 1 bar of CO_2) have now shown that under these conditions the 1,3-AS in fact follows the concerted pathway to an appreciable extent (Reimann, B.; Sadler, D. E.; Schaffner, K., unpublished results).

(22) Schuster, D. I.; Underwood, G. R.; Knudsen, T. P. *J. Am. Chem. Soc.* **1971**, *93*, 4304.

(23) Houk, K. N.; Northington, D. J.; Duke, R. E., Jr. *J. Am. Chem. Soc.* **1972**, *94*, 6233.

(24) Del Bene, J.; Jaffé, H. H. *J. Chem. Phys.* **1968**, *48*, 1807, 4050.

(25) Houk, K. N. *Chem. Rev.* **1976**, *78*, 1.

(26) It is interesting to note in this context that, e.g., in a 3-phenyl-substituted β,γ-UK of type **1**[2b,c] the phosphorescence of the $T_1(\pi,\pi^*)$ state is practically indistinguishable from that of the parent triplet π system, 1-phenylcyclopentene. In other words, the mixing-in of the n,π^* configuration remains below the limit of spectral detection in this case.

(27) Pople, J. A. *J. Chem. Phys.* **1965**, *43*, S129.

Table VI. Dependence of the Fluorescence Yield for Ketones **1a-c** on Solvent Polarity

ketone	$\varphi_{f(rel)}$[a] C_8H_{18}	$\varphi_{f(rel)}$[a] MTHF[b]	$k_{f(C_8H_{18})}/k_{f(MTHF)}$[a,c]
1a	1.0	0.58	0.99
1b	1.0	0.69	0.93
1c	1.0	0.80	0.98

[a] Solvents: C_8H_{18}, isooctane; MTHF, 2-methyltetrahydrofuran. For Φ_f see ref 21. [b] Relative to $\varphi_{f(rel)}$ in C_8H_{18} = 1.0. [c] $k_{f(C_8H_{18})}/k_{f(MTHF)} = \Phi_{f(C_8H_{18})} \times \tau_{f(MTHF)}/\tau_{f(C_8H_{18})} \times \Phi_{f(MTHF)}$.

of 5°, 10°, and 15° were considered. The state energies of the ground state strongly increased with increasing twist angle. Roughly the same behavior was also found for the $^3(n,\pi^*)$ state, while the energy increase was substantially smaller in the $^3(\pi,\pi^*)$ state. This latter result can be interpreted as a superimposition of a resistance owing to ring strain and the energy decrease of olefins in the π,π^* states. The η values showed the same trend also in the twisted conformations, but with the η for nonbonded C(2)–CO interaction in the $^3(\pi,\pi^*)$ state increasing significantly more strongly with the twisting. At a 15° twist the increase was 36% relative to the twisted ground state.

From these semiempirical calculations conclusions can be drawn about the electronic structure of the molecule at or very near to the equilibrium geometry. It is quite clear, on the one hand, that in both the $^1(n,\pi^*)$ and $^3(n,\pi^*)$ states the α cleavage of the C(1)–CO bond is more likely to occur than in the $^3(\pi,\pi^*)$ state. On the other hand, decoupling of the π bond by twisting around the C=C double bond is more favored in the $^3(\pi,\pi^*)$ state than in the other states considered. The weakening of the π bond is accompanied by enhanced nonbonded interaction between C(2) and the carbonyl carbon.

In summary we may note that the theoretical calculations described above are in full accord with the stereochemistry- and multiplicity-dependent mechanistic scheme derived from our previous studies of the photochemistry of these β,γ-UK systems[2] and from the experimental results described in this work.[7]

Comparison of the Kinetic Data with Literature Results

Activation energy barriers for the α cleavage reaction of ketones have only been determined in a very few cases. Turro et al.[28] have measured values of ca. 5 kcal/mol for two bicyclo[2.2.1]heptan-2-ones in which α cleavage is the major process deactivating S_1. It seems plausible that in both this and our system the activation barriers are associated with a stretching of the C_α–CO bond.

It is of particular interest to compare our results with the kinetic investigation by Schuster and Calcaterra[29] of the closely related β,γ-UK **17**. This study represents an important contribution to the understanding of β,γ-UK photochemistry. An activation barrier of ≤4 kcal/mol was measured for the pathway leading to the 1,3-AS product, as shown by increasing quantum yields for the 1,3-AS reaction with increasing temperature. However, in contrast to **1a–c** (cf. Tables III and VI) there is no effect of solvent polarity on the magnitude of this activation barrier, as shown by the invariance of Φ_f for **17** on changing the solvent from cyclohexane to acetonitrile.[30]

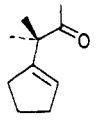

17

The claim[31] that the 1,3-AS from $T_2(n,\pi^*)$ of **17** has no activation barrier because the quantum yields for the sensitized 1,3-AS reaction do not vary with temperature need not necessarily be true. If T_2 is predominantly deactivated by one temperature-activated process, which leads in part to the 1,3-AS product, then any change in the rate constant for the reaction would be matched by an approximately equal and opposite change in the lifetime of T_2, resulting in no change in the quantum yield for the reaction despite possibly large variations in the rate constant. That this may well be the case is suggested by the elegant xenon perturbation experiments[29] which show that internal conversion to T_1 in **17** is very inefficient.

Experimental Section

IR spectra, recorded on a Perkin-Elmer 700 infrared spectrometer with $CHCl_3$ solutions, are reported in cm^{-1}. The abbreviations used are as follows: st (strong), me (medium), w (weak), b (broad). ^1H NMR spectra were measured in $CDCl_3$, with $(CH_3)_4Si$ as an internal standard, at 60, 80, and 270 MHz on Bruker WH 60E, WP 80, and WH 270 instruments, respectively. The chemical shifts are given in δ values, and the coupling constants (J) are in Hz (abbreviations: s (singlet), d (doublet), t (triplet), q (quadruplet), and m (multiplet)). MS spectra were run on a Varian MAT CH 5 instrument.

Gas chromatographic (GC) analyses were carried out on OV 101 glass capillary columns (20 and 35 m), unless otherwise state, with a flame ionization detector coupled to an electronic integrator.

Synthesis of 1,2-Dimethyl-3-trideuteriomethylcyclopent-2-enyl Methyl Ketone (1d). Ethyl 1-Trideuteriomethyl-2-oxocyclopentanecarboxylate (5). A solution of ethyl 2-oxocyclopentanecarboxylate (**4**; 65.5 g, 0.42 mol) in t-BuOH (400 mL) and CD_3I (69.6 g, 0.48 mol) were added consecutively to a solution of t-BuOK (47.1 g, 0.42 mol) in t-BuOH (500 mL). After being stirred for 2 days at room temperature, the mixture was concentrated to ca. 300 mL and the precipitate was filtered off and washed with ether. The solution and the washings were combined, concentrated to ca. 300 mL, added to 300 mL of CH_2Cl_2, and washed with saturated aqueous NH_4Cl. Fractional distillation gave **5** (67.8 g, 93% yield): IR 1755, 1725 (both st); NMR 1.25 (3 H, t, J = 7) and 4.15 (2 H, q, J = 7) OC_2H_5, ca. 2.0 and 2.3 (6 H, two m) $(CH_2)_3$; MS 173 ($C_9H_{11}O_3D_3$, M^+), 145, 128, 72 (base peak).

Ethyl 3-Trideuteriomethyl-2-oxocyclopentanecarboxylate (6). Treatment of **5** (67.8 g, 0.39 mol) with Na in EtOH and toluene following the method of Sisido et al.[32] gave **6** (54.7 g, 81% yield) after fractional distillation: IR 1755, 1725 (both st); NMR 1.30 (3 H, t, J = 7) and 4.20 (2 H, q, J = 7) OC_2H_5, ca. 2.3 (5 H, m) $(CH_2)_2CH$, ca. 3.2 (1 H, m) CH; MS 173 ($C_9H_{11}O_3D_3$, M^+), 145, 127, 99 (base peak).

Ethyl 1-Methyl-3-trideuteriomethyl-2-oxocyclopentanecarboxylate (7). Methylation of **6** (54.7 g, 0.32 mol) with t-BuOK (35.5 g, 0.32 mol) and CH_3I (50.8 g, 0.36 mol) as above gave **7** (55.3 g, 95% yield): IR 1755, 1725 (both st); NMR 1.26 (3 H, s) CH_3, 1.25 (3 H, t, J = 7) and 4.25 (2 H, q, J = 7) OC_2H_5, ca. 1.5–2.5 (5 H, m) $(CH_2)_2CH$; MS 187 ($C_{10}H_{13}O_3D_3$, M^+), 159 (base peak), 142, 130, 114.

Mixture of Diastereoisomeric Ethyl 2-Hydroxy-1,2-dimethyl-3-trideuteriomethylcyclopentanecarboxylates (8). A Grignard reaction of **7** (55.3 g, 0.30 mol) with CH_3MgI prepared from Mg (9.1 g, 0.40 mol) and CH_3I (52.3 g, 0.37 mol) in dry ether (300 mL) afforded, after fractional distillation, **8** (56.1 g, 94% yield): IR 3500 (b), 1720 (st); NMR 1.10 (3 H, t) and ca. 4.2 (2 H, m) OC_2H_5, 1.20 (6 H, s) two CH_3, ca. 1.6–2.5 (5 H, m) $(CH_2)_2CH$; MS 203 ($C_{11}H_{17}O_3D_3$, M^+), 188, 129 (base peak).

Ethyl 1,2-Dimethyl-3-trideuteriomethylcyclopent-2-enecarboxylate (9). Dehydration[2c] of **8** (56.1 g, 0.28 mol) with p-toluenesulfonic acid in

(28) Mirbach, M. F.; Mirbach, M. J.; Liu, K.-C.; Turro, N. J. *J. Photochem.* **1978**, *8*, 299.

(29) Schuster, D. I.; Calcaterra, L. T. *J. Am. Chem. Soc.* **1982**, *104*, 6397.

(30) This interpretation requires the assumption that k_f is invariant with solvent polarity. We have shown this to be the case for the β,γ-UKs **1a–c** (Table VI).

(31) The uncertainties inherent in interpreting quantum yields as opposed to rate constants are further illustrated for **17** by the study of the triplet-sensitized quantum yields for the 1,3-AS and ODPM reactions. While the ratios of the quantum yields are meaningful, their absolute values cannot be interpreted directly. As Schuster and Calcaterra[29] state, these values depend on the efficiency with which the triplet states of **17** are populated. Under the experimental conditions used, namely one single concentration of **17**, the efficiency of quenching and thus the efficiency of reaction would be expected to vary as a function of sensitizer triplet lifetime, since it cannot be assumed that the sensitizer would be totally quenched. Even if conditions for apparent total quenching of the sensitizer were established, by determining the quantum yields as a function of concentration of **17**, it would still not be possible to distinguish between different quenching rates—reflecting different triplet energies—and partitioning after an initial exciplex quenching encounter. The interpretation of these processes requires rate data. It is of interest to note in this context that the rate constants for the 1,3-AS reaction of **1a–c** give good Arrhenius fits (Figure 3), while the quantum yields (Table IV) show an irregular dependence on temperature.

(32) Sisido, K.; Utimoto, K.; Isida, T. *J. Org. Chem.* **1964**, *29*, 2781.

benzene gave **9** (48.3 g, 95% yield): IR 3030 (w), 1725 (st); NMR 1.25 (3 H, s) and 1.6 (3 H, m) two CH_3, 1.20 (3 H, t, J = 7) and 4.10 (2 H, q, J = 7) OC_2H_5, ca. 2.3 (4 H, m) $(CH_2)_2$; MS 185 ($C_{11}H_{15}O_2D_3$, M^+), 159, 142, 130, 112 (base peak).

1,2-Dimethyl-3-trideuterioethylcyclopent-2-enecarboxylic Acid (10). Hydrolysis[2c] of **9** (48.3 g, 0.27 mol) with KOH in aqueous MeOH gave **10** (30.0 g, 74% yield): IR 2500–3500 (b), 1690 (st); NMR 1.26 (3 H, s) and ca. 1.6 (3 H, m) two CH_3, ca. 2.4 (4 H, m) $(CH_2)_2$, 12.0 (1 H, s) CO_2H; MS 157 ($C_9H_{11}O_2D_3$, M^+), 112 (base peak).

Methylation[2c] of **10** (10.0 g, 0.065 mol) with 90 mL of a standardized 1.64 M solution of CH_3Li (0.15 mol) in ether gave **1d** (6.5 g, 65% yield): IR 3040 (w), 1705 (s); NMR 1.10, 2.05 (each 3 H, s), and 1.45 (3 H, m) three CH_3, ca. 2.4 (4 H, m) $(CH_2)_2$; MS 155 ($C_{10}H_{13}OD_3$, M^+), 140, 112 (base peak).

Synthesis of 1-Trideuteriomethyl-2,3-dimethylcyclopent-2-enyl Methyl Ketone (2d). 1-Trideuteriomethyl-2,3-dimethylcyclopent-2-enecarboxylic Acid (12). The conversion of **4** (53.3 g, 0.34 mol) to **12** (21.7 g, 41% yield) was effected by the steps outlined above for the synthesis of **10**, rather than following the different procedure employed previously[14] for the preparation of **11**. **12**: IR 2500–3500 (b), 1690 (st); NMR 1.6 (6 H, m) two CH_3, ca. 2.3 (4 H, m) $(CH_2)_2$, 12.0 (1 H, s) CO_2H; MS 157 ($C_9H_{11}O_2D_3$, M^+), 112 (base peak).

Methylation[2c] of **12** (10.0 g, 0.064 mol) with CH_3Li (0.15 mol) gave **2d** (8.9 g, 90% yield): IR 3040 (w), 1705 (st); NMR 1.45, 1.75 (each 3 H, m) and 2.05 (3 H, s) three CH_3, ca. 2.4 (4 H, m) $(CH_2)_2$; MS 155 ($C_{10}H_{13}OD_3$, M^+), 112 (base peak).

Enantiomeric Resolution of Ketones (±)-1d and (±)-2d. Preparation of the Diastereoisomeric Acetals 14, 14′, 15, and 15′. To a solution of (±)-**1d** (3.3 g, 25 mmol) and (*S*)-(−)-2,3-butanediol (3.5 g, 39 mmol; Fluka) in benzene (100 mL) was added dry *p*-toluenesulfonic acid (10 mg). The mixture was refluxed for 4.5 h with a fitted Dean and Stark head and water condenser. The solution was then stirred three times each for 15 min with 100 mL of H_2O, dried, and concentrated to yield essentially pure **14**/**14′** (5.19 g, 93% yield): NMR ca. 1.2 (9 H, m) and ca. 1.5 (6 H, m) five CH_3, ca. 1.5–2.1 (4 H, m) $(CH_2)_2$, ca. 3.6 (2 H, m) two CH; MS 227 (M^+, $C_{14}H_{21}O_2D_3$ − 15), 115 (base peak).

The acetals **15** and **15′** were prepared from (±)-**2d** as above: NMR 1.05 (3 H, s), 1.2 (9 H, m), and 1.5 (3 H, m) five CH_3, ca. 1.5–2.1 (4 H, m) $(CH_2)_2$, ca. 3.6 (2 H, m) two CH; MS 227 and 224 (M^+, $C_{14}H_{21}O_2D_3$ − 15 and 18, respectively), 115 (base peak).

Separation of the Diastereoisomeric Acetals. A typical separation of 3 g of a 50:50 mixture of **14**/**14′** or **15**/**15′** by chromatography over a column of 150 g of silica gel (70–230 mesh), eluting with 1:1 benzene–hexane (125 mL fractions), yielded 70:30 (0.8 g), 50:50 (1.6 g), and 30:70 (0.6 g) mixtures over 13 fractions (by GC, PPG 70-m glass capillary column). Repeated chromatography afforded the desired degree of enrichment (85:15 and 15:85).

Hydrolysis of the Acetals. In a typical experiment **14**/**14′** (0.48 g, 2.1 mmol) was dissolved in EtOH (15 mL), 10% HCl (3 mL) added, and the mixture stirred at room temperature for 6 h. The workup with ether, aqueous $NaHCO_3$, and H_2O furnished a light yellow oil (0.31 g) which gave essentially pure **1d** (0.30 g, 90% yield) after filtration through silica gel (9 g, 70–230 mesh) eluting with 100 mL of 10% ether in CH_2Cl_2.

Determination of the Enantiomeric Composition of 1d and 2d. Typically, the addition of 50–80 mg of praseodymium tris(*D*-3-heptafluorobutyrylcamphorate) [Pr(hfc)$_3$; Lancaster Synthesis, Ltd.] was required to separate the quaternary methyl signals of (+)- and (−)-**1d** (ca. 10 mg in ca. 0.6 mL of $CDCl_3$) and to determine their relative amounts by planimetry. Spectral separation and resolution were best between 30 and 50 °C. The separated signals were assigned to the appropriate enantiomers by comparison with the optical rotation.[2a,15]

The enantiomeric composition of **2d** was determined by GC analysis (PPG 70-m glass capillary column) of the diastereoisomeric acetals before hydrolysis. Comparison in one case of the GC analysis of the acetals with NMR optishift and optical rotation measurements of the enantiomeric ratio of the ketones produced on hydrolysis showed agreement to within ±2%: GC 29.39/70.61 (average of three measurements); NMR 31.1/68.9, 30.7/69.3; optical rotations 31.5 (+)/68.5 (−) (measured on a Perkin-Elmer 241 polarimeter), 31.0 (+)/69.0 (-) (Zeiss OLD 5 polarimeter).

Irradiation of the (+)-Ketones 1a and 1b. Determination of the Quantum Yields of Reaction to 2a,b and to 3a,b. Argon-purged solutions of 0.01–0.02 M ketone in isooctane or 2-methyltetrahydrofuran (with *n*-nonane or *m*-xylene as an internal GC standard) were irradiated at 313 nm in an electronically integrating actinometer[33] with magnetic stirring. A variable-temperature cuvette was used for the temperature-dependence studies. The products **1d** + **2d** (not separable by GC) and **3d**[2a,b] in the irradiated solution were determined by GC (44-m OV 7 glass capillary column). The actinometer was calibrated with use of potassium ferrioxalate actinometry.[34]

Irradiation of the Enantiomerically Enriched Ketones 1d and 2d. Determination of the Quantum Yields of Reaction (1,3-AS and ODPM Rearrangement to 3d) and Change in the Ratio of the Enantiomers of 1d in CH_3OH as a Function of Temperature. Argon-purged solutions of 0.06–0.08 M ketone in CH_3OH (with *m*-xylene as an internal GC standard) were irradiated at 313 nm as described above. In this case, however, it was necessary to combine in the analytical procedure GC (65-m OV 101 glass capillary columns) and NMR measurements. For the ^1H NMR (80 MHz) measurements the mixtures of **1d** + **2d** were isolated (ca. 10 mg) by preparative GC and then dissolved in ca. 0.6 mL of $CDCl_3$. The absolute amounts of **1d** and **2d** were calculated from the ratio **1d**/**2d** obtained from integration of the quaternary and acetyl methyl signals, in conjunction with the analytical GC data. Addition of optishift reagent then allowed the ratio of the enantiomers of **1d** to be determined.

The quantum-yield determination of reaction of (±)-**1d** at 20 °C in isooctane were performed as described above for the enantiomerically enriched ketone.

Fluorescence Lifetime Measurements. The measurements were carried out by using the single-photon-timing technique.[35] The excitation source was a synchronously pumped mode-locked and cavity-dumped dye laser system (Spectra-Physics) with rhodamine 6G as the dye. The output pulses of the dye laser were frequency doubled in a KDP crystal of 1.5-mm thickness. The excitation wavelength was 303 nm. The fluorescence was selected by a double monochromator with 8-nm bandwidth. A photomultiplier with a multialkali photocathode in a cooled housing was used for detection. The width of the apparatus function, as measured from a dilute Ludox scatterer, was ca. 220 ps (full width at half maximum). The laser pulse intensities used to measure the fluorescence decays were less than 10^{10} photons/cm^2 with a repetition rate of 400 kHz. About 5000 counts were routinely collected in the peak channel. The glass optics in the emission monochromator did not allow the determination of the prompt response at 303 nm. Instead that at 606 nm (nondoubled) was used, limiting the accurate determination of lifetimes to those greater than ca. 200 ps.

During the measurements a Leybold VSK_4-300 flow cryostat served to maintain the sample temperature constant within ±2 °C. The temperature was measured with a PT 100 resistor.

The τ_0 values (i.e., the reciprocal of the sums of the temperature-independent rate constants; cf. Figures 1 and 2) were extrapolated to 0 K from the lifetimes measured down to 60 K.

Registry No. 1a, 68752-16-9; **1b**, 70987-82-5; **1c**, 70987-81-4; (±)-**1d**, 88928-94-3; (+)-**1d**, 85312-99-8; (−)-**1d**, 85313-00-4; (±)-**2d**, 88928-93-2; (+)-**2d**, 85313-01-5; (−)-**2d**, 85313-02-6; (±)-**4**, 53229-92-8; (±)-**5**, 88867-71-4; **6**, 88867-72-5; **7**, 88867-73-6; **8**, 88867-74-7; (±)-**9**, 88867-75-8; (±)-**10**, 88928-91-0; (±)-**11**, 88867-76-9; (±)-**12**, 88928-92-1; (−)-**13**, 19132-06-0; **14**, 88867-77-0; **14′**, 88867-78-1; **15**, 88867-79-2; **15′**, 88867-80-5.

(33) Amrein, W.; Gloor, J.; Schaffner, K. *Chimia* **1974**, *28*, 185.
(34) Hatchard, C. G.; Parker, C. A. *Proc. R. Soc. London, Ser. A* **1956**, *235*, 518. Demas, J. N.; Bowman, W. D.; Zalewski, E. F.; Velapoldi, R. A. *J. Phys. Chem.* **1981**, *85*, 2766.
(35) Holzwarth, A. R. *Laser Optoelektr.* **1982**, *14*, 39. Ware, W. R.; Pratinidhi, M.; Bauer, R. K. *Rev. Sci. Instrum.* **1983**, *54*, 1148.